



Compressed Sensing-Based Direct Conversion Receiver

Pierzchlewski, Jacek; Arildsen, Thomas; Larsen, Torben

Published in:
2012 International Symposium on Communications and Information Technologies (ISCIT)

DOI (link to publication from Publisher):
[10.1109/ISCIT.2012.6381012](https://doi.org/10.1109/ISCIT.2012.6381012)

Publication date:
2012

Document Version
Accepted author manuscript, peer reviewed version

[Link to publication from Aalborg University](#)

Citation for published version (APA):
Pierzchlewski, J., Arildsen, T., & Larsen, T. (2012). Compressed Sensing-Based Direct Conversion Receiver. In *2012 International Symposium on Communications and Information Technologies (ISCIT)* (pp. 804 - 809). IEEE Press. <https://doi.org/10.1109/ISCIT.2012.6381012>

General rights

Copyright and moral rights for the publications made accessible in the public portal are retained by the authors and/or other copyright owners and it is a condition of accessing publications that users recognise and abide by the legal requirements associated with these rights.

- Users may download and print one copy of any publication from the public portal for the purpose of private study or research.
- You may not further distribute the material or use it for any profit-making activity or commercial gain
- You may freely distribute the URL identifying the publication in the public portal -

Take down policy

If you believe that this document breaches copyright please contact us at vbn@aub.aau.dk providing details, and we will remove access to the work immediately and investigate your claim.

Compressed Sensing-Based Direct Conversion Receiver

Jacek Pierzchlewski, Thomas Arildsen and Torben Larsen

Aalborg University

Faculty of Engineering and Science

Department of Electronic Systems

Niels Jernes Vej 12, 9000 Aalborg, Denmark

jap@es.aau.dk, tha@es.aau.dk, tl@es.aau.dk

Abstract—Due to the continuously increasing computational power of modern data receivers it is possible to move more and more processing from the analog to the digital domain. This paper presents a compressed sensing approach to relaxing the analog filtering requirements prior to the ADCs in a direct conversion receiver. In the presented solution, the filtered down-converted radio signals are randomly sampled with an average sampling frequency lower than its Nyquist rate, and then reconstructed in a DSP system. To enable compressed sensing, this approach exploits the frequency domain sparsity of the down-converted radio signals.

As shown in an experiment presented in the article, when the proposed method is used, it is possible to relax the requirements for the quadrature down-converter filters. A random sampling device and an additional digital signal processing module is the price to pay for these relaxed filter requirements.

Index Terms—data receiver, receiver digitization, Software Defined Radio, compressed sensing, random sampling, down-converter

I. INTRODUCTION

Twenty years ago around 98% of the radio frequency communication receivers were heterodyne [1], but the cost-driven evolution dethroned heterodyne receivers from this position. At present, direct conversion receivers [1], [3], [4] are widely used in mobile devices, though heterodyne receivers are still used in more expensive equipment due to superior performance. There are many disadvantages of the direct conversion receiver architecture [3], [4], of which the most important is sensitivity to distortion produced by strong interfering signals, spurious leakage of local oscillators, DC offset after the mixer, mismatching between in-phase and quadrature-phase signals and generally poor sensitivity. Nevertheless, direct conversion receivers consist of significantly less analog elements than heterodyne receivers, which makes them cheaper and more suitable for integration.

The current challenge is to relax the requirements for the analog parts of a direct conversion receiver, due to design and integration problems which are caused by the analog parts. New possibilities for solving this problem appear with increasing computational power available in receivers. The present paper investigates the problem of relaxing the requirements for the quadrature down-converter filters. In the direct-conversion receivers there are high requirements for the down-conversion filters due to noise, interference, and

high frequencies generated by the down-conversion process. These filters cause challenges in integration, mostly due to IC (Integrated Circuit) area required to implement these filters. Recently there was proposed a direct conversion circuit in which uniform sampling is replaced with a pseudorandom sampling technique [6]–[8]. Afterwards, the sampled signal is reconstructed in a DSP (Digital Signal Processing) system. Hence, a minor reduction of the order of the quadrature down-converter filters was possible.

In the presented solution, the frequency domain sparsity of a down-converted signal is exploited. In this paper the authors propose to randomly sample the down-converted signals with an average frequency lower than the Nyquist rate of the signal. Then, a reconstruction of the down-converted signals is performed using compressed sensing reconstruction algorithms. Compressed sensing is a signal processing technique which allows sampling of a signal below its Nyquist rate and, under certain assumptions, recover the signal afterwards using a reconstruction algorithm [9]–[12]. To make a compressed sensing process possible, the sampled signal must be compressible. A signal is compressible if it is possible to approximate this signal in some domain with a sparse vector. In this paper the authors show that the down-converted radio signal is sparse in the frequency domain and hence, it can be compressively sampled. A random sampler which acquires the signal and a modified reconstruction method is presented. Hence to the proposed solution, the down-converted radio signal can be compressively sampled without a high order post-mixer low-pass filter. A random sampling process and an additional DSP module is the price pay in order to enable the proposed modifications.

The paper is organized as follows. The problem of the down-converter filters and the idea of the compressed sensing-based homodyne receiver is presented in Section II. A practical experiment is presented in section III. Finally, some conclusions are presented in section IV.

II. COMPRESSED SENSING-BASED DIRECT CONVERSION RECEIVER

A. Quadrature down-converter filters in a direct conversion receiver

A typical direct conversion receiver dedicated to digital communication is presented in Fig. 1. A radio frequency signal

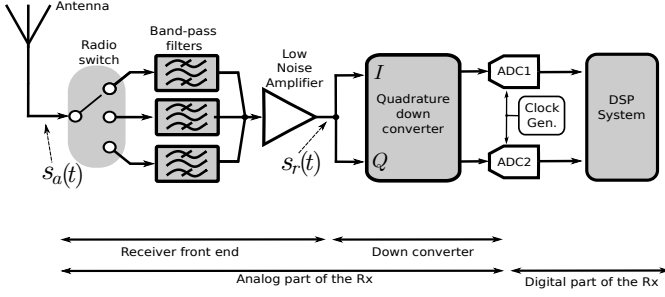


Fig. 1: The analog and the digital part of a direct conversion receiver

from the antenna is filtered by a bank of RF band-pass filters, which selects the currently received band, and amplified by a low noise amplifier. The filtered radio frequency signal $s_r(t)$ is:

$$s_r(t) = s(t) + s_b(t) + n_r(t) \quad (1)$$

where $s(t)$ is the wanted radio signal to be received:

$$s(t) = I(t) \cdot \cos(2\pi f_0 t) - Q(t) \cdot \sin(2\pi f_0 t) \quad (2)$$

where f_0 is the carrier frequency, $I(t)$ and $Q(t)$ are transmitted information-carrying band-limited signals. The non-bandlimited noise $n_r(t)$ in (1) represents all analog noise (including noise from the entire receiver, the channel and from the transmitter). The $s_b(t)$ component in (1) represents adjacent channel interference signals (blockers) present in the filtered radio signals due to the size of frequency spectrum allowed by the band-pass radio filters (Fig. 2):

$$s_b(t) = s_{b1}(t) + s_{b2}(t) + \dots + s_{bN}(t) \quad (3)$$

where N is the current number of blockers. The frequency range of the radio filter pass-band is $[f_0 - f_r, f_0 + f_r]$. The blockers are distributed somewhere in this spectrum, neither the number of blockers nor their exact frequency distribution is known.

The filtered radio frequency signal is processed by a quadrature down-converter circuit. In the down-converter (Fig. 3) the radio frequency signal is split into I and Q , and mixed with a signal of a frequency equal to the radio carrier frequency f_0 . This process separates the bandpass signal (1) into a low-frequency component ($\lambda_I(t)$ in the I -path and $\lambda_Q(t)$ in the

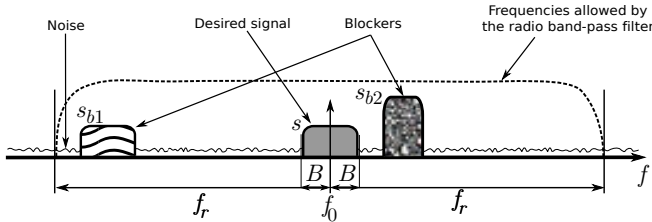
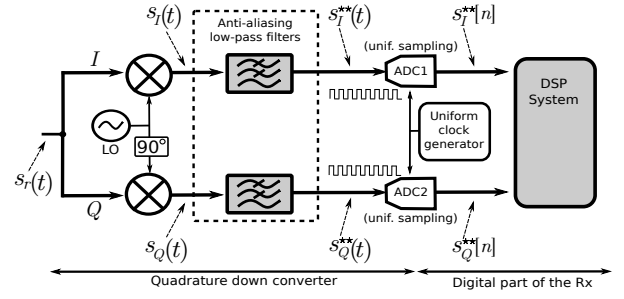
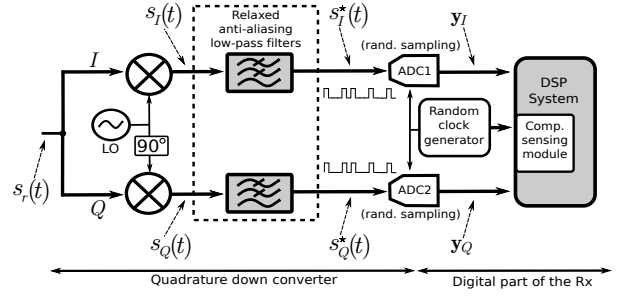


Fig. 2: The filtered radio signal s_r in the frequency domain. Beside of the desired signal there are blockers in the signal spectrum, due to wide frequency range allowed by the radio filter



(a) Conventional quadrature down-converter, samplers and a DSP system in a direct conversion receiver



(b) Proposed compressed-sensing based quadrature down-converter with relaxed anti-aliasing filters, random samplers and a DSP system in a direct conversion receiver

Fig. 3: Conventional and proposed down-converter, samplers and DSP System in a direct conversion receiver

Q -path) and high frequency component ($X_I(t)$ in the I -path and $X_Q(t)$ in the Q -path):

$$s_I(t) = \lambda_I(t) + X_I(t) + n_I(t) \quad (4)$$

$$s_Q(t) = \lambda_Q(t) + X_Q(t) + n_Q(t) \quad (5)$$

where $s_I(t)$ and $s_Q(t)$ are the down-converted signals in the I and Q respectively (Fig. 3a). In the above equation, the $n_I(t)$ and $n_Q(t)$ represent the non-bandlimited noise. The low-frequency components $\lambda_I(t)$ and $\lambda_Q(t)$ consist of wanted information-carrying band-limited signals $I(t)$ and $Q(t)$, and unwanted low-frequency down-converted blockers:

$$\lambda_I(t) = \frac{1}{2} \cdot I(t) + \underbrace{b_{I1}(t) + \dots + b_{IN}(t)}_{\text{Blockers in the } I \text{ path}} \quad (6)$$

$$\lambda_Q(t) = \frac{1}{2} \cdot Q(t) + \underbrace{b_{Q1}(t) + \dots + b_{QN}(t)}_{\text{Blockers in the } Q \text{ path}} \quad (7)$$

In the current paper, it is assumed that there is no co-channel interference, so the blockers are distributed in the frequency domain from the wanted signal baseband B until the f_r ($[f_0 + B, f_0 + f_r]$) (Fig. 4).

In the conventional direct conversion receivers the down-converted signals $s_I(t)$ and $s_Q(t)$ are filtered by high-order low-pass filters (Fig. 3a) which remove the high frequency components X_I and X_Q , virtually all the noise and the downconverted blockers (Fig. 4). It can be stated that in the above case the filtered signals s_I^{**} and s_Q^{**} consist of only the

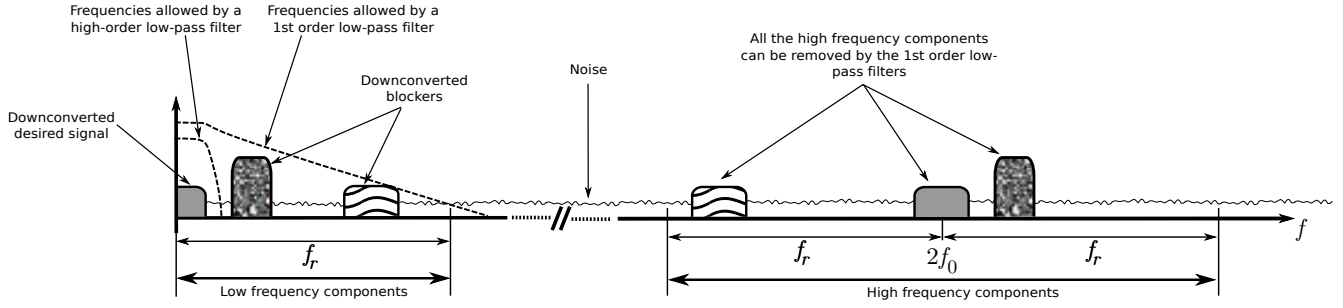


Fig. 4: The downconverted signal in the frequency domain

information carrying band-limited signals $I(t)$ and $Q(t)$:

$$s_I^{**} = \frac{1}{2}I(t), \quad s_Q^{**} = \frac{1}{2}Q(t) \quad (8)$$

The filtered signals $s_I^{**}(t)$ and $s_Q^{**}(t)$ are then uniformly sampled by ADCs:

$$s_I^{**}[n] = s_I^{**}\left(n\frac{1}{f_u}\right), \quad s_Q^{**}[n] = s_Q^{**}\left(n\frac{1}{f_u}\right), \quad n \in \mathbb{N} \quad (9)$$

where f_u is the uniform sampling frequency which must be higher than the Nyquist frequency of the band-limited signals $I(t)$ and $Q(t)$. Eventually, discrete signals $s_I^{**}[n]$ and $s_Q^{**}[n]$ are processed by the DSP hardware. In this paper it is assumed that there is no I/Q imbalance in the receiver [17].

The low-pass anti-aliasing quadrature down-converter filters need to be of a high order, which creates severe problems in IC implementation. This is due to the chip area occupancy and the needed accuracy in filter design. Relaxing requirements for these filters without quality loss in a received signal is a problem which attracts more and more attention in radio communication engineering [6]–[8].

B. Low-order filters in homodyne receivers

In the presented solution the high order low-pass filters are replaced by 1st order low-pass filters (Fig. 3b). With this filter the high-frequency components X_I and X_Q and most of the noise are removed. The downconverted blockers are still present in the filtered signal (Fig. 4). The signals filtered with a 1st order low-pass filter s_I^* and s_Q^* are:

$$s_I^*(t) = \frac{1}{2} \cdot I(t) + \underbrace{b_{I1}^*(t) + \dots + b_{IN}^*(t)}_{\text{Filtered blockers (I path)}} + n_I^*(t) \quad (10)$$

$$s_Q^*(t) = \frac{1}{2} \cdot Q(t) + \underbrace{b_{Q1}^*(t) + \dots + b_{QN}^*(t)}_{\text{Filtered blockers (Q path)}} + n_Q^*(t) \quad (11)$$

where $n_I^*(t)$ and $n_Q^*(t)$ reflect the noise present in the filtered signal. Due to the fact that blockers present in the signal may be distributed in the frequency domain until the frequency f_r (Fig. 4), the sampling rate needed to acquire the filtered signals $s_I^*(t)$ and $s_Q^*(t)$ is significantly higher than the sampling frequency needed to acquire the signals $s_I^{**}(t)$ and $s_Q^{**}(t)$ from (9). Implementation of Analog-to-Digital Converters (ADCs) which operate at such a high sampling frequency is impractical due to huge energy dissipation, and is virtually impossible in many applications.

C. Compressed sensing methodology

Let us consider a continuous analog signal $x(t)$, $0 \leq t \leq t_x$ with the highest frequency component B and the Nyquist frequency $f_N = 2B$. A given signal $x(t)$ is sampled:

$$\mathbf{y} = \phi(x(t)) \quad (12)$$

where ϕ represents the signal sampling process, $\mathbf{y} \in \mathbb{R}^{M \times 1}$ is a discrete observed signal. Let us assume that the average sampling rate f_s of the observed signal \mathbf{y} is lower than the Nyquist frequency f_N of the sampled signal $x(t)$:

$$f_s = \frac{M}{t_x}, \quad f_s < f_N \quad (13)$$

where t_x is the time length of the signal $x(t)$. According to the compressed sensing theory [9]–[11], under certain conditions it is possible to reconstruct the vector $\mathbf{x} \in \mathbb{C}^{N \times 1}$, from the undersampled observed signal \mathbf{y} . The vector \mathbf{x} is a discrete model of the sampled signal $x(t)$:

$$\mathbf{x}[n] = x(nT_r), \quad T_r = \frac{1}{f_r}, \quad f_r > f_N \quad (14)$$

The reconstruction is performed with a reconstruction procedure $\mathcal{R} : \mathbf{y} \rightarrow \mathbf{x}$. The sampling frequency f_r of the discrete reconstructed signal \mathbf{x} is higher than the average sampling frequency f_s and higher than the Nyquist rate f_N of the signal $x(t)$.

The first condition which must be fulfilled to enable compressed sensing is that the sampled signal $x(t)$ is compressible. The signal $x(t)$ is compressible if its discrete model \mathbf{x} can be approximated in a given domain $\Psi \in \mathbb{C}^{N \times K}$, $K \leq N$ with a sparse vector $\mathbf{v} \in \mathbb{C}^K$:

$$\mathbf{x} \approx \Psi \mathbf{v}, \quad \|\mathbf{v}\|_0 < K \quad (15)$$

where the 'zero norm' [9] describes the number of non-zero elements in the vector. The more sparse the vector \mathbf{v} is, the lower sampling frequency f_s is needed to successfully reconstruct the discrete signal \mathbf{x} [9], [10]. Using the vector \mathbf{x} it is possible to represent the acquisition procedure ϕ with a measurement matrix $\Phi \in \mathbb{R}^{M \times N}$:

$$\mathbf{y} = \Phi \mathbf{x} \quad (16)$$

The relation between the sparse vector and the observed vector may be expressed as:

$$\mathbf{y} = \Theta \mathbf{v}, \quad \Theta = \Phi \Psi, \quad \Theta \in \mathbb{C}^{M \times K} \quad (17)$$

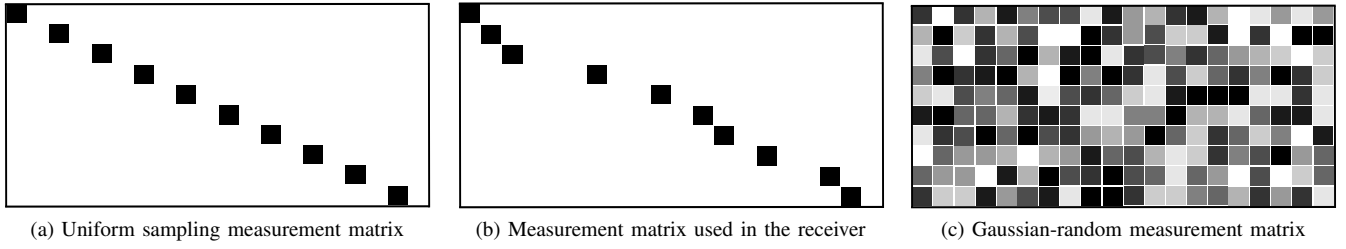


Fig. 5: Comparison of different measurement matrices Φ . The measurement matrix used in the experiment is a compromise between the randomness in the sampling process and the complexity of the acquisition device

D. Sampler

The Restricted Isometry Property (RIP) was introduced in [10]. This property denotes, how close the matrix $\Theta = \Phi\Psi$ behaves like an orthonormal matrix if the vector \mathbf{v} is K -sparse (only K entries of the vector are non-zero). It was showed in [12] that if the measurement matrix Φ is a random matrix, then the matrix $\Theta = \Phi\Psi$ fulfills the requirement of Restricted Isometry Property (RIP) for most of the possible sparse vectors. Therefore, the sampling process should be maximally randomized to ensure the correct signal reconstruction. In practical signal sensing circuits it is, however, nontrivial to comply with the demand of randomness. The random demodulator [15] is a well-known single-ADC solution for compressed sensing signal acquisition. Unfortunately, the random demodulator contains a multiple-order low-pass filter. Furthermore, imperfections of this filter may severely influence the signal reconstruction [16]. Due to these drawbacks, usage of the Random Demodulator is unacceptable in the considered application.

In the following system we use a random sampler following the post-mixer filters in the quadrature down-converter. The sampler does not include any preconditioning in the derivations to follow. In a practical context it may be necessary with conditioning as always to ensure that the input signals comply with the dynamic range of the sampler and following quantizer. The compressed sensing system processes the sampled signal in blocks of length t_B . The moments in which the signal is acquired are gathered in a sampling pattern set \mathbb{S} :

$$\mathbb{S} = \{t_1, t_2, \dots, t_M\} \quad t_M \leq t_B \quad (18)$$

Let us introduce a sampling grid set \mathbb{G} :

$$\mathbb{G} = \{\tau_1, \tau_2, \dots, \tau_K\}, \quad \tau_k = kT_g \quad (19)$$

where T_g is a sampling grid period. The sampling pattern is always a subset of the grid set $\mathbb{S} \subset \mathbb{G}$. In other words, the sampling moments can occur only at multiples of the sampling grid period T_g . Therefore, the sampling grid period describes the resolution of sampling. The average sampling ratio f_s is:

$$f_s = \frac{N_s}{t_B} \quad (20)$$

where N_s is the number of samples in a sampling pattern. The sampling grid period T_g is shorter than the shortest time between adjacent signal sampling moments required by the ADC used in the system. It can be stated that $T_g \leq T_{\min} \leq T_s$ where T_s is the average sampling period. The

sampling patterns are generated such that the minimum time between sampling moments T_{\min} is kept. An example of a measurement matrix Φ is compared to a Gaussian random measurement matrix and a uniform sampling measurement matrix in Fig. 5. The matrix generated by the proposed random sampler contains sufficient level of randomness, as it is shown later in numerical experiments.

E. Signal reconstruction procedure

The filtered signals $s_I^*(t)$ and $s_Q^*(t)$ can be approximated as sparse in the frequency domain (Fig. 4). Therefore, the dictionary $\Psi \in \mathbb{C}^{N \times K}$ used in the experiment is the discrete Fourier transform dictionary:

$$\Psi = [\psi_1, \psi_2, \dots, \psi_K] \quad (21)$$

where a column ψ_k of the dictionary matrix corresponds to a tone of frequency $k\gamma$, where γ is frequency separation between dictionary tones. A column ψ_k of the dictionary matrix:

$$\psi_k = \cos(2k\pi n T_r) + j \cdot \sin(2k\pi n T_r) \quad (22)$$

where $n \in \{1, \dots, N\}$, T_r is the sampling period of the reconstructed signal. The frequency separation γ depends on the time length of the processed signal t_B :

$$\gamma < \frac{1}{t_B} \quad (23)$$

In the proposed reconstruction γ is set to

$$\gamma = \frac{1}{2t_B} \quad (24)$$

The highest tone used in the receiver depends on the maximum frequency component which may be found in the signals filtered with a 1st-order low-pass filter:

$$K = \frac{f_r}{\gamma} \quad (25)$$

The signal reconstruction algorithms are based on the ℓ_1 optimization procedure:

$$\mathcal{R}_I : \mathbf{v}_I = \min \|\hat{\mathbf{v}}_I\|_1 \quad \text{sub. to : } \|\mathbf{y}_I - \Phi_I \text{Re}(\Psi \hat{\mathbf{v}}_I)\|_2 < \epsilon_I \quad (26)$$

$$\mathcal{R}_Q : \mathbf{v}_Q = \min \|\hat{\mathbf{v}}_Q\|_1 \quad \text{sub. to : } \|\mathbf{y}_Q - \Phi_Q \text{Re}(\Psi \hat{\mathbf{v}}_Q)\|_2 < \epsilon_Q \quad (27)$$

where \mathcal{R}_I and \mathcal{R}_Q are the reconstruction procedures for the I - and Q -paths respectively. The matrices Φ_I and Φ_Q are the measurements matrices which reflect the randomized sampling process in the I - and Q -paths. The parameters ϵ_I and ϵ_Q relax

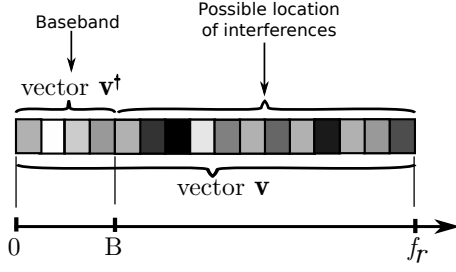


Fig. 6: The vector with frequency coefficients which covers the range $[0, f_r]$ is used in the convex optimization procedures (26) and (27). The vector \mathbf{v}^\dagger is used in final reconstruction (28)

the feasible area of optimization due to noise present in the observed signal. These parameters should be adjusted to the current level of noise. The vectors \mathbf{y}_I and \mathbf{y}_Q are the signals observed in the I - and Q -paths.

The \mathbf{v}_I and \mathbf{v}_Q are the reconstructed vectors of frequency coefficients (Fig. 6). The discrete representation of the wanted information-carrying baseband signals I_r and Q_r is reconstructed as

$$I_r = \Psi^\dagger \mathbf{v}_I^\dagger, \quad Q_r = \Psi^\dagger \mathbf{v}_Q^\dagger \quad (28)$$

where $\mathbf{v}_I^\dagger \in \mathbb{C}^{K^\dagger \times 1}$ and $\mathbf{v}_Q^\dagger \in \mathbb{C}^{K^\dagger \times 1}$ are the truncated reconstructed vectors of frequency coefficients. These vectors contain only the frequency coefficients which correspond to the frequencies of the wanted information-carrying signals I and Q :

$$\mathbf{v}_I^\dagger(k) = \mathbf{v}_I(k), \quad \mathbf{v}_Q^\dagger(k) = \mathbf{v}_Q(k) \quad (29)$$

where $k = \{1, \dots, K^\dagger\}$. The index K^\dagger is:

$$K^\dagger = \frac{B}{\gamma} \quad (30)$$

where B is the bandwidth of the signals I and Q . The dictionary $\Psi^\dagger \in \mathbb{C}^{N \times K^\dagger}$ is the truncated dictionary used in the reconstruction:

$$\Psi^\dagger = [\psi_1, \psi_2, \dots, \psi_{K^\dagger}] \quad (31)$$

III. NUMERICAL EXPERIMENT

The numerical experiment was conducted to test the presented concept. The experiment is presented in Fig. 7. The time of the simulation is $t_s = 10 \mu\text{s}$. In the experiment white Gaussian noise signals are transmitted as the I and Q signals. The baseband of the I and Q signals is $B = 3 \text{ MHz}$, the average power is $P_B = 1 \text{ W}$ each. The I and Q signals are upconverted to a bandpass radio signal s_{tx} with a carrier frequency $f_0 = 800 \text{ MHz}$. The power P_{tx} of the radio signal s_{tx} is 1 W . The signal is summed with interference signal s_{int} . The s_{int} signal consists of 10 continuous wave signals:

$$s_{int} = \sum_{i=1}^{10} a_i \cos(2\pi f_i t) \quad (32)$$

where the frequencies f_i of the interfered signals are in the range $(f_0 - f_r \leq f_i \leq f_0 - B)$ or $(f_0 + B \leq f_i \leq f_0 + f_r)$.

There are two possible bandwidths considered, within which the interfering signals are contained: $f_r = 40 \text{ MHz}$ and $f_r = 80 \text{ MHz}$. Two levels of the power P_{int} of the interference signal s_{int} considered in the experiment: $P_{int} = 0.1 \text{ W}$ and $P_{int} = 1 \text{ W}$. The received radio signal s_r is amplified, downconverted and filtered with a 1st order low-pass filter with a cut-off frequency $f_{-3dB} = 20 \text{ MHz}$. The filtered baseband signals are polluted with white Gaussian noise signals. There are 6 levels of noise power considered in the experiment (SNR_n): 10 dB , 15 dB , 20 dB , 25 dB , 30 dB , 35 dB , 40 dB where

$$SNR_n = \frac{P^*}{P_n} \quad (33)$$

where P^* is the power of the filtered signal, P_n is the power of noise signals n_I and n_Q . The baseband signals are sampled by a random sampler with the average random sampling frequency $f_s = 30 \text{ MHz}$, which corresponds to oversampling $OSR = 0.375$ and $OSR = 0.1875$ for the size of two possible frequency ranges given by $f_r = 40 \text{ MHz}$ and $f_r = 80 \text{ MHz}$ respectively. The baseband signals are reconstructed with the compressed sensing reconstruction method described in II-E. The reconstructed signals I_r and Q_r are compared to the original baseband signals I and Q . For evaluation purposes, the average power of each of the reconstructed signals I_r and Q_r is adjusted to P_B (1 W). Before the comparison, the reconstructed signals are shifted in time to compensate delays introduced by the filters. The time shift is set experimentally. Both the reconstructed and the original signals are windowed with the Tukey window to suppress effects of numerical errors at the beginning and at the end of the reconstructed signal. The error vectors e_I and e_Q are computed:

$$e_I = I_r^w - I^w, \quad e_Q = Q_r^w - Q^w \quad (34)$$

where I_r^w and Q_r^w are the time-shifted and windowed reconstructed baseband signals, the I^w and Q^w are the windowed original baseband signals. The signal-to-noise ratios of the reconstructed baseband signals are:

$$SNR_I = \frac{P_{I^w}}{P_{e_I}}, \quad SNR_Q = \frac{P_{Q^w}}{P_{e_Q}} \quad (35)$$

where P_{I^w} and P_{Q^w} are the power of the windowed original signals I^w and Q^w respectively. The P_{e_I} and P_{e_Q} are the power of the error vectors e_I and e_Q signals respectively. The average of the values SNR_I and SNR_Q is treated as the measure of the reconstruction quality:

$$SNR_r = \frac{1}{2}(SNR_I + SNR_Q) \quad (36)$$

The results of the experiment are shown in Fig. 8. As it can be seen in Fig. 8 the baseband signal can be reconstructed in adverse conditions even if 1st order low-pass filters are used as the quadrature down-converter filters. As expected, the less polluted with noise, the better reconstruction is achieved. The 10 dB increase of the power of interference causes $5\text{--}6 \text{ dB}$ loss in the reconstruction. For the lower value of the size of the possible frequency range which must be checked for interference ($f_r = 40 \text{ MHz}$) the baseband signal reconstruction quality is $2\text{--}3 \text{ dB}$ better than in the case of wider frequency range ($f_r = 80 \text{ MHz}$).

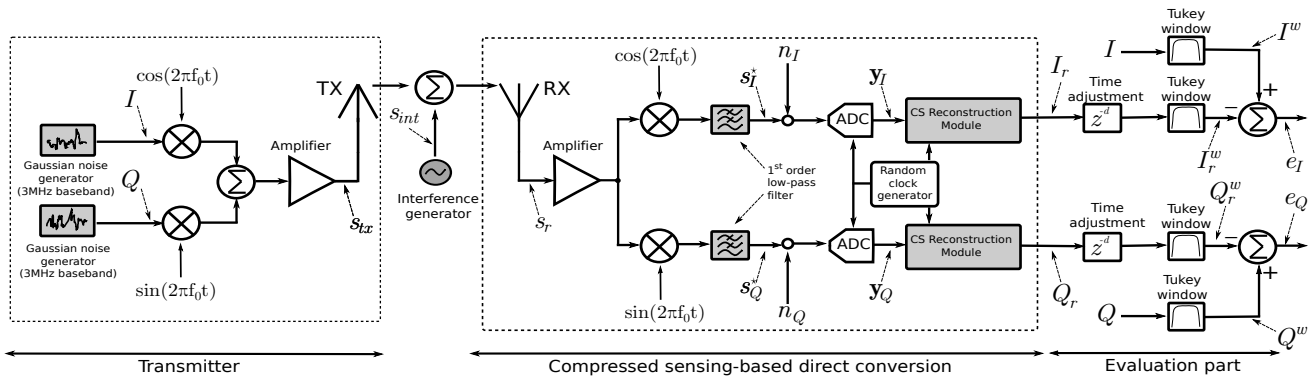


Fig. 7: The conducted numerical experiment

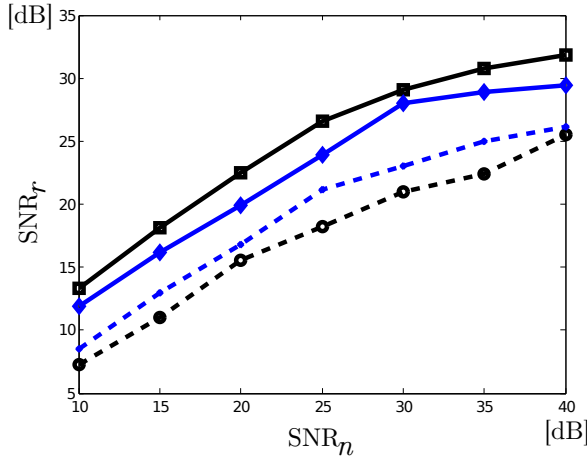


Fig. 8: Results of the experiment. Reconstructed signal SNR_r plotted vs. noise SNR_n . The range of the interference is $f_r = 40\text{MHz}$ and $f_r = 80\text{MHz}$. The power of interference is $P_{in} = 1\text{ W}$ and $P_{in} = 0.1\text{ W}$. ($f_r = 40\text{ MHz}$ $P_{in} = 1\text{ W}$: \circ , $f_r = 80\text{ MHz}$ $P_{in} = 1\text{ W}$: \diamond , $f_r = 80\text{ MHz}$ $P_{in} = 0.1\text{ W}$: \square , $f_r = 40\text{ MHz}$ $P_{in} = 0.1\text{ W}$: \circ)

IV. CONCLUSIONS

In this paper, a modified architecture for direct conversion radio receivers is proposed. The architecture is based on compressed sensing principles. It is shown that the proposed solution enables relaxing the requirements for the order of the quadrature filters in a direct conversion receiver. An experiment is presented in which the transmitted quadrature signal is polluted with noise and interference. The experiment demonstrates that the proposed architecture is able to successfully receive the baseband signal under adverse conditions with the usually high-order quadrature filters reduced to first-order filters.

ACKNOWLEDGMENT

This work is supported by The Danish National Advanced Technology Foundation under grant number 035-2009-2 and The Danish Council for Strategic Research under grant number 09-067056.

REFERENCES

- [1] A. A. Abidi, "Direct-Conversion Radio Transceivers for Digital Communications", *IEEE J. Solid-State Circuits*, vol. 30, no 12, pp. 1399-1410, Dec. 1995.
- [2] A. A. Abidi, "The Path to the Software-Defined Radio Receiver", *IEEE J. Solid-State Circuits*, vol. 30, no 12, pp. 1399-1410, Dec. 2007.
- [3] B. Razavi, "Architectures and Circuits for RF CMOS Receivers.", *Proc. of IEEE 1998 Custom Integrated Circuits Conference*, pp. 393400, Santa Clara, USA, May 1998.
- [4] Besser, L. and Gilmore, R., "Practical RF Circuit Design for Modern Wireless Systems.", *Artech House 2003*, ISBN 1-58053-521-6, Norwood, USA
- [5] N. C. Davies, "A high performance HF software radio", *Proc. 8th Int. Conf. HF Radio Systems and Techniques*, Guildford, UK, pp. 249-256, 2000
- [6] M. Ben-Romdhane, C. Rebai, P. Desgreys, A. Ghazeli, P. Loumeau, "Flexible Baseband Analog Front-end for NUS based Multistandard Receiver", *Proc. Joint IEEE North-East Workshop on Circuits and Systems and TAISA Conference*, Toulouse, France, pp. 1-4, June 2009.
- [7] M. Ben-Romdhane, C. Rebai, P. Desgreys, A. Ghazeli, P. Loumeau, "Pseudorandom Clock Signal Generation for Data Conversion in a Multistandard Receiver", *Proc. IEEE Int. Conference on Design and Technology of Integrated Systems in Nanoscale Era*, pp. 14, Tozeur, Tunisia, Mar. 2008.
- [8] M. Ben-Romdhane, C. Rebai, K. Grati, A. Ghazeli, G. Hechmi, P. Desgreys and P. Loumeau, "Non-Uniform Sampled Signal Reconstruction for Multistandard WiMax/WiFi Receiver", *IEEE International Conference on Signal Processing and Communication*, pp. 181184, Dubai, November 2007.
- [9] E.J. Candès and M. B. Wakin, "An Introduction To Compressive Sampling", *IEEE Signal Process. Mag.*, vol. 25(2), pp. 21-30, Mar. 2008.
- [10] E.J. Candès and T. Tao, "Decoding by Linear Programming", *IEEE Trans. Inf. Theory*, vol. 51(12), pp. 4203-4215, Nov. 2005.
- [11] E.J. Candès, J. Romberg and T. Tao, "Robust Uncertainty Principles: Exact Signal Reconstruction From Highly Incomplete Frequency Information", *IEEE Trans. Inf. Theory*, vol. 52(2), pp. 489-509, Feb. 2006.
- [12] R.G. Baraniuk, M. Davenport, R. Devore, M. Wakin, "A Simple Proof of the Restricted Isometry Property for Random Matrices", *Constructive Approximation*, vol. 28(3), pp. 253-236, 2008.
- [13] J.A. Tropp, "Just Relax: Convex Programming Methods for Identifying Sparse Signals in Noise", *IEEE Trans. Inf. Theory*, vol. 52(3), pp. 1030-1051, Mar. 2006.
- [14] J.A. Tropp and A.C. Gilbert, "Signal Recovery From Random Measurements Via Orthogonal Matching Pursuit", *IEEE Trans. Inf. Theory*, vol. 53(12), pp. 4655-4666, Dec. 2007.
- [15] S. Kirolos, J. Laska, M. Wakin, M. Duarte, D. Baron, T. Ragheb, Y. Massoud, R. Baraniuk, "Analog-to-Information Conversion via Random Demodulation", *Proc. IEEE Dallas/CAS Workshop on Design Applications Integration and Software (DCAS)*, pp. 71-74, Dallas, USA, 2006.
- [16] P. J. Pankiewicz, T. Arildsen, T. Larsen, "Sensitivity of the random demodulation framework to filter tolerances", *Proc. 19th European Signal Processing Conference (EUSIPCO)*, pp. 534-538, Barcelona, Spain, 2011.
- [17] Y. Zhou, Z. Pan, "Impact of LPF Mismatch on I/Q Imbalance in Direct Conversion Receivers", *IEEE Trans. Wireless Commun.*, vol. 10(4), pp. 1702-1708, Jun. 2011.